Biophysical Journal, Volume *114*

Supplemental Information

Stochastic Model of Maturation and Vesicular Exchange in Cellular Organelles

Quentin Vagne and Pierre Sens

Stochastic Model of Maturation and Vesicular Exchange in Cellular Organelles

Supporting Material

Quentin Vagne[1] and Pierre Sens[1]

[1]Institut Curie, PSL Research University, CNRS, UMR 168, 23 rue d'Ulm, F-75005, Paris, France.

December 19, 2017

In this Supporting Material, we derive the recursion relation for the mean first passage time to complete compartment maturation, we show how to obtain the mean-field approximation of the stochastic compartment dynamics, we give details of the numerical procedure used for the simulations, and we provide additional simulation results.

S1 Recursion relation

We start by deriving the classical equation on mean first passage times for a discrete one dimensional system submitted to a stochastic dynamics governed by transition rates. We consider a system described by a discrete variable $n \in \mathbb{N}$. The dynamics of n is stochastic and the transition rate from the configuration n to another configuration m is written $R_{n\to m}$. We are interested in the quantity τ_n which is the average time needed to reach the configuration 0 starting from configuration n. We call $p(n,t)dt$ the probability to reach 0 between t and $t+dt$ starting from n at $t=0$. One can write an equation on the functions $p(n,t)$ by computing the probability to reach 0 at time $t+dt$ starting from n. In order to do this, during a time dt the system will either jump towards another configuration m or stay in n and then use a time t to reach the configuration 0. Mathematically written, it reads:

$$p(n,t+dt) = \sum_{m\neq n} R_{n\to m}dt\ p(m,t) + \left(1 - \sum_{m\neq n} R_{n\to m}dt\right) p(n,t) \tag{S1}$$

This leads to a differential equation on $p(n,t)$:

$$\frac{\partial p(n)}{\partial t} = \sum_{m\neq n} R_{n\to m}(p(m,t) - p(n,t)) \tag{S2}$$

Multiplying by t and integrating on the time leads to an equation for the mean first passage time τ_n to reach $n=0$ starting at n, which a classical result obtained in [1] p298-303 in the restricted

case of one-step processes:

$$\forall n \in \mathbb{N} : \ -1 = \sum_{m \neq n} R_{n \to m}(\tau_m - \tau_n). \tag{S3}$$

This recursion relation is used is the main text (Eq.(9)) to compute the mean first passage time to full maturation, Eq.(11).

S2 Mean-field approximation of the compartment dynamics

The (inherently stochastic) compartment dynamics is defined by Eq.2 from the main text:

$$\begin{aligned}
\text{Fusion} : \ & (N_A, N_B) \to (N_A + n_v, N_B) \text{ at rate } J(N, \phi) \\
\text{Maturation} : \ & (N_A, N_B) \to (N_A - 1, N_B + 1) \text{ at rate } k_m(\phi) N_A \\
\text{Budding} : \ & (N_A, N_B) \to (N_A, N_B - n_v) \text{ at rate } K(\phi) N_B \quad \text{if } N_B \geq n_v \\
& (N_A, N_B) \to (N_A, 0) \text{ at rate } K(\phi) N_B \quad \text{if } N_B < n_v
\end{aligned} \tag{S4}$$

The compartment also contains a neutral species contributing to its total size N. Hence, for completeness, we need to explicitly define the dynamics of N:

$$\begin{aligned}
\text{Fusion} : \ & N \to N + N_v \text{ at rate } J(N, \phi) \\
\text{Budding} : \ & N \to N - N_v \text{ at rate } K(\phi) N_B \quad \text{if } N_B \geq n_v \\
& N \to N - N_v \text{ at rate } K(\phi) N_B \quad \text{if } N_B < n_v
\end{aligned} \tag{S5}$$

From this set of stochastic equations, a first step towards constructing a mean-field approximation is to compute the time derivative of the average quantities N,N_A and N_B:

$$\begin{aligned}
\langle \dot{N} \rangle =& N_v \langle J(N, \phi) \rangle - N_v \langle K(\phi) N_B \rangle \\
\langle \dot{N_A} \rangle =& n_v \langle J(N, \phi) \rangle - \langle k_m(\phi) N_A \rangle \\
\langle \dot{N_B} \rangle =& \langle k_m(\phi) N_A \rangle - n_v P_{N_B \geq n_v} \langle K(\phi) N_B \rangle_{N_B \geq n_v} - P_{N_B \geq n_v} \langle K(\phi) {N_B}^2 \rangle_{N_B < n_v}
\end{aligned} \tag{S6}$$

Where, $\forall t \geq 0$, $\langle X \rangle_Y$ is the (ensemble) average value of $X(t)$ given constraint Y, and P_Y is the probability that constraint Y is verified at time t. It is important to note Eq.(S6) is a direct consequence from Eq.(S4) and Eq.(S5) and is therefore exact. Now to obtain a mean-field approximation, one traditionally replaces every average of products or non-linear combinations of variables by products or combinations of the averages. Also fluctuations are neglected so $P_{N_B \geq n_v}$ is taken equal to 1 when $\langle N_B \rangle \geq n_v$. This leads to the following complete mean-field equation:

$$\begin{aligned}
\dot{N} =& N_v (J(N, \phi) - K(\phi) N_B) \\
\dot{N_A} =& n_v J(N, \phi) - k_m(\phi) N_A \\
\dot{N_B} =& k_m(\phi) N_A - n_v K(\phi) N_B \text{ if } N_B \geq n_v \\
\dot{N_B} =& k_m(\phi) N_A - K(\phi) {N_B}^2 \text{ if } N_B < n_v
\end{aligned} \tag{S7}$$

Because of the change of behavior when $N_B < n_v$, the general solution of this system is complex. The mean-field equations are generally valid for large systems when fluctuations can be neglected. In such cases we can assume that $N_B \geq n_v$. In this case we can easily relate $\dot{N}$ and $\dot{N_A} + \dot{N_B}$:

$$\frac{\dot{N}}{N_v} = \frac{\dot{N_A} + \dot{N_B}}{n_v} \tag{S8}$$

From this we conclude that the relation $(N_A + N_B)/N = n_v/N_v$ is valid for all time, provided that it is verified at $t = 0$. This allows to derive the self-consistent equations for the mean-field steady-state:

$$\frac{N}{N_v} = \frac{N_A + N_B}{n_v} = \frac{J(N,\phi)}{(1-\phi)k_m(\phi)} \qquad \phi = \frac{k_m(\phi)}{k_m(\phi) + K(\phi)n_v} \tag{S9}$$

This corresponds to Eq.4 of the main text.

S3 First passage time for a deterministic maturation process

In the main text, maturation of a single site is assumed to be a single step process. In reality the maturation mechanism might involve several steps. As a consequence the distribution of the maturation time of a given component would be different from a single exponential. The limit where maturation involves a large number of independent steps can be discussed relatively easily. Because of the central limit theorem, the distribution of the total maturation time of a single component is expected to be a Gaussian with a relatively small standard deviation. The extreme case is when the number of steps goes to infinity and the maturation is deterministic. We can compute the first passage time to full maturation of the compartment in this case. We choose the value $1/k_m$ for the deterministic maturation time of a single component in order to compare with the result of the main text. Here each site of type A has a lifetime $1/k_m$, therefore full maturation occurs only if no new vesicle is injected during a time $1/k_m$ after the injection of the last vesicle. Vesicles are injected at a rate J in the simplified model, and each injection completely resets the maturation state of the system. Since vesicle injections are independent, this leads to this expression for the average maturation time τ:

$$\tau = \frac{1}{k_m} + \langle n_{inj}\rangle \langle t_{inj}\rangle \tag{S10}$$

where $\langle n_{inj}\rangle$ is the average number of vesicle injections in addition to the first one and $\langle t_{inj}\rangle$ is the average waiting time between two injections. In order to compute these two quantities, we define the survival probability $p_S(t)$ which is the probability to reach the time t without injecting a vesicle. The equation satisfied by $p_S(t)$, and its solution, are:

$$\frac{dp_S}{dt} = -Jp_S(t)\ , \qquad p_S(t) = e^{-Jt} \tag{S11}$$

The probability of reaching $t = 1/k_m$ without experiencing a vesicle injection (a reset) is $p_0 \equiv p_S(1/k_m)$, hence the probability of experiencing exactly n jumps before complete separation is $p_n = p_0(1-p_0)^n$. Consequently, the mean number of jumps is

$$\langle n_{inj}\rangle = \sum_{n=1}^{\infty} np_n = \frac{1-p_0}{p_0} \tag{S12}$$

For one reset event, the probability density of the reset time is $-\frac{dp_S}{dt}$ so the average waiting time before a vesicle injection is given by:

$$\langle t_{inj}\rangle = \frac{\displaystyle\int_0^{1/k_m} t\frac{dp_S}{dt}dt}{\displaystyle\int_0^{1/k_m} \frac{dp_S}{dt}dt} = \frac{-p_0/k_m + \displaystyle\int_0^{1/k_m} p_S(t)dt}{1-p_0} \tag{S13}$$

Introducing Eqs.(S12,S13) in Eq.(S10), we get the expression of the separation time:

$$\tau = \frac{1}{p_S(1/k_m)} \int_0^{1/k_m} p_S(t)dt = \frac{e^{\frac{J}{k_m}} - 1}{J} \tag{S14}$$

This is exactly the same result as in the main text where maturation is made of a single step (Eq.(11)), which suggests that as long as the injection of new vesicle can be treated as a Poisson process, the first passage time to full maturation should not be affected much by the actual distribution of the maturation time of single components.

S4 Simulation scheme

S4.1 General framework

We make use of the Gillepie algorithm [2] to perform exact stochastic simulations of our system. The Gillespie algorithm is a general method that allows to compute statistically correct trajectories for a stochastic system. The system must be described by a discrete set S of states. Being in a given state $i \in S$ at time t, the system must have a probability $R_{i\to j}dt$ to jump from i to another state j between t and $t+dt$. This definition is rather general, which allows the Gillespie algorithm to be applied in a variety of Physical contexts. Here the state space S is composed of all the possible configurations of the compartment. A single state is defined as a couple (N_A, N_B) (or equivalently (N, ϕ) with $N = N_A + N_B$ and $\phi = N_B/N$) in which N_A and N_B are the numbers of A sites and B sites in the compartment. Below is the list of all the allowed transitions between states together with their transition rates:

$$\begin{aligned}
\text{Fusion}: &\ (N_A, N_B) \to (N_A + n_v, N_B) \text{ at rate } J(N, \phi) \\
\text{Maturation}: &\ (N_A, N_B) \to (N_A - 1, N_B + 1) \text{ at rate } k_m(\phi) N_A \\
\text{Budding}: &\ (N_A, N_B) \to (N_A, N_B - \min(n_v, N_B)) \text{ at rate } K(\phi) N_B
\end{aligned} \tag{S15}$$

Where the functions $J(N, \phi)$, $k_m(\phi)$ and $K(\phi)$ can be arbitrary but must remain positive. After defining the system and its dynamics, the Gillespie algorithm can be employed to generate statistically exact trajectories using the following scheme:

1. Initialize a random number generator.
2. Initialize the system at $t = 0$ in a state Ω. Here we choose the state $\Omega = (n_v, 0)$, meaning that we start with a single vesicle of type A as a compartment.
3. Compute the sum Σ of all the transition rates out of the state Ω, and use it to generate the waiting time Δt before the next event using the distribution $\Sigma e^{-\Delta t \Sigma}$.
4. Choose randomly the state Ω' reached after Δt from the list of possible states, knowing that the probability of having $\Omega \to \Omega'$ is given by $R_{\Omega\to\Omega'}/\Sigma$.
5. Update the time to $t + \Delta t$ and the state Ω accordingly with whatever event has been selected.
6. Loop back to step 3.

This scheme has been proved to generate trajectories that are exact in the sense that the probability for the program to generate a given trajectory is equal to the probability of observing this trajectory in the real system. In this paper we implemented this algorithm in the C language using the Mersenne-Twister pseudo random number generator.

S4.2 Construction of the phase diagram

We aim at computing the value of the parameter η defined in the main text. In order to compute this quantity we need to obtain average values for N_{ves} the total number of emitted vesicles and N_{mat} the final size of the compartment after complete maturation. We therefore performed a large number of simulations all identical apart from the initial state of the random number generator. We initialize the system at $t = 0$ with $(N_A, N_B, N_{ves}) = (n_v, 0, 0)$ and let the simulation run. After each time step we increase N_{ves} if a vesicle budding has happened and check for complete maturation which is defined by $N_A = 0$. Once complete maturation or a maximum number of simulation steps is reached the simulation is stopped. N_{ves} is registered together with the final size N_{mat} of the compartment. We perform 320 of these simulations (for each set of parameters) and we require that at least 90% of them went to full maturation to compute satisfying estimates of the average values $\langle N_{ves} \rangle$ and $\langle N_{mat} \rangle$ (see error bars on Fig.3 - main text). This gives the value of η for a specific value of J, k_m and K, which corresponds to one point in the phase diagram of Fig.3 in the main text. The process is then repeated in an automated way to compute the value of η for all the 20x20 points. For certain points (small values of ϕ_B and/or large values of N), less than 90% of the simulations get to full maturation. We therefore cannot precisely compute η but we verified that we always had $\eta > 0.99$. The value of η displayed on Fig.3 for these points is arbitrarily set to 1.

S5 Additional results

S5.1 Phase diagram for constant rates

In Fig.2 of the main text the phase diagram for the transition between the vesicular export dominated regime and the compartment maturation dominated regime is presented as a function of the quasi-steady-state values of the compartment size and composition. This is to ease the comparison between the different models, for which a given steady-state corresponds to different values of the kinetic rates. For completeness, we present in Fig.S1 the same phase diagram as a function of the model parameters J/K and k_m/K.

As discussed in the text, the size distribution of mature compartment presents a peak at small size in the basic model. This corresponds to the direct maturation of small compartments with a size comparable to that of a single vesicle. This contribution is due to the fact that our model does not include any specific process for the nucleation of a compartment and the initiation of maturation. To see the influence of direct maturation on the output parameter η, we present in Fig.S1c modified output parameters where direct maturation events have been removed, and where all events for which the fully matured compartment is of unit size (because of direct maturation or following several fusion and budding events), have been removed. It shows that these types of events do not qualitatively modify the picture, and make a quantitative difference only for very small steady-state compartment size.

S5.2 Scatter plots for the outflux

The output parameter η is computed using the average of N_{ves} and N_{mat} over many simulations, and therefore brings no information on the fluctuations of these quantities. These fluctuations are shown as scatter plots of N_{ves} and N_{mat} on Fig.S2a for constant rates and Fig.S2b with homotypic fusion. The distribution of the values can be understood using mean-field arguments. Assuming

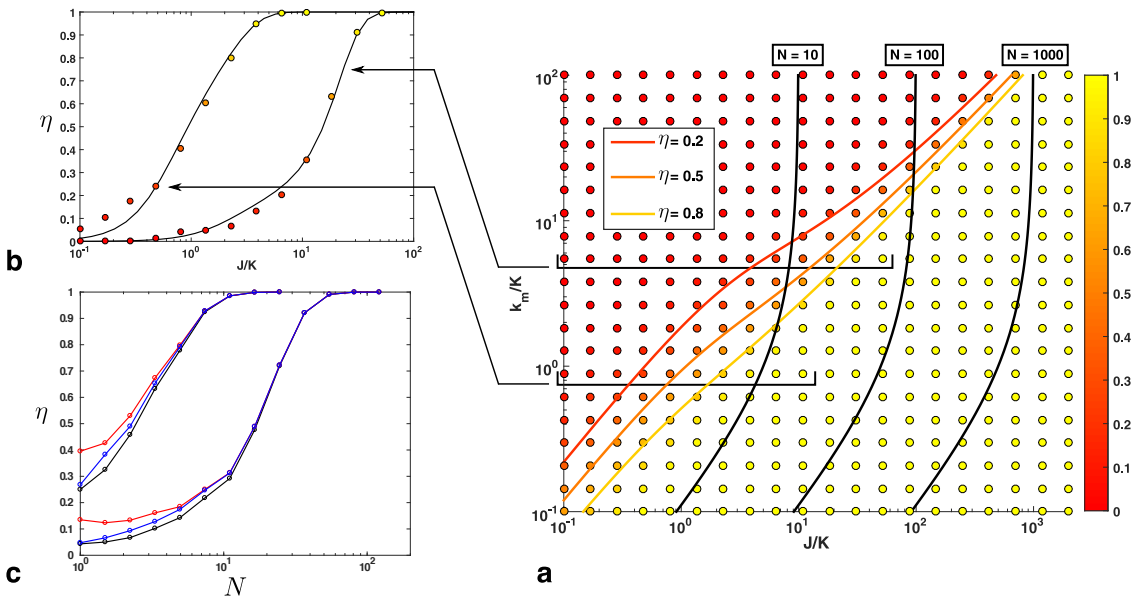

Figure S1: Simulation results. **a**. Phase diagram: the value of the output parameter η as a function of the in-flux J and maturation rate k_m, normalized by the budding rate K, illustrates the transition between the *vesicular exchange* ($\eta \simeq 1$) and *compartment maturation* ($\eta \simeq 0$) regimes. The black lines show constant values of the compartment size in the pseudo steady-state (Eq.4 - main text). The three colored lines represent constant values of η as given by the approximate analytical computation of Eq.12 - main text. **b**. Cuts through the phase diagram varying the compartment size for two fixed pseudo steady-state compositions. **c**. Output parameter as a function of the steady-state compartment size for two values of the steady-state composition N_B/N_A, as in Fig.2c of the main text. The black curves includes all possible events and is identical to the curves of Fig.2c. For the red curve, all direct maturation of a compartment, prior to any fusion event, have been removed. For the blue curve, all events where the fully matured compartment is of unit size, either because of direct maturation or after fusion and budding events, have been removed.

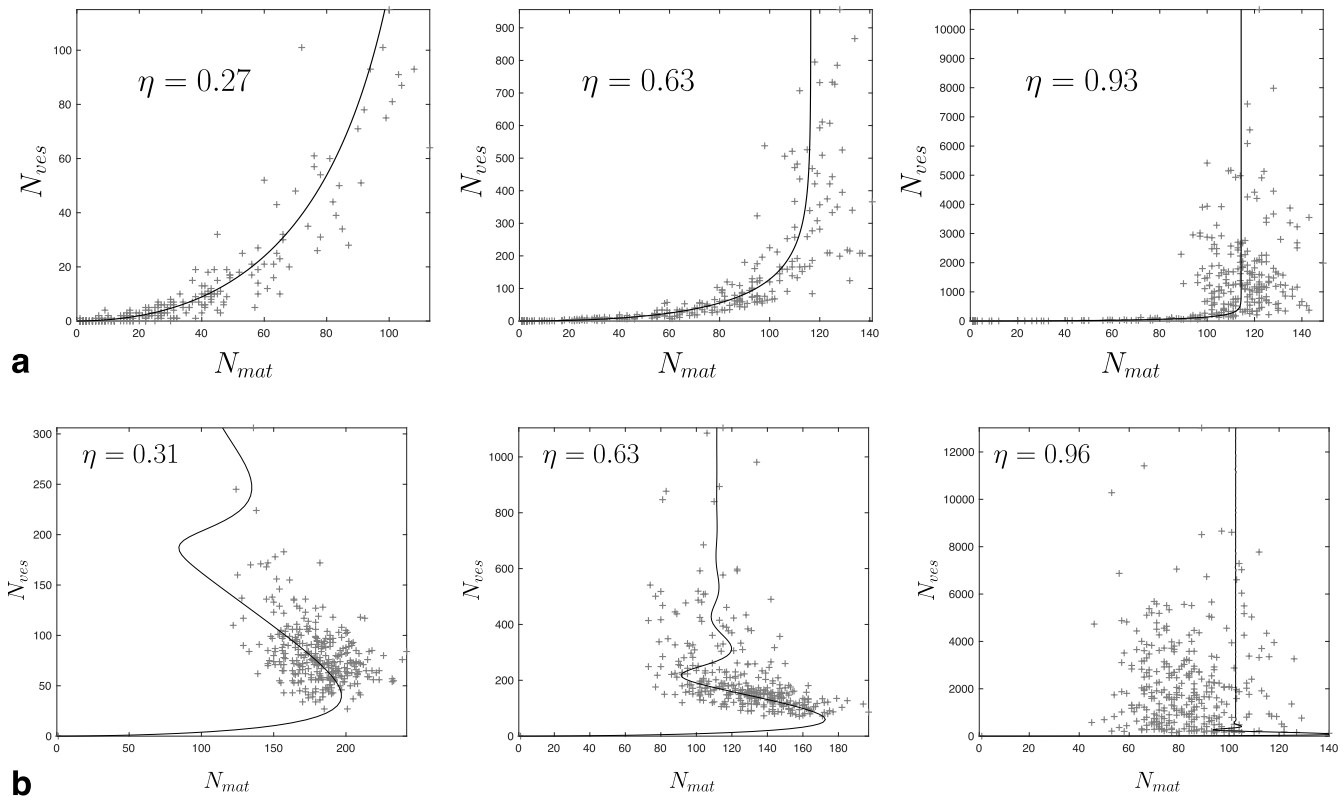

Figure S2: Scatter plots for the distributions of N_{ves} and N_{mat} (crosses) obtained from 320 independent simulations (for three different values of η) for **a.** a constant influx and **b.** a composition-dependent influx $J \sim (1-\phi)$. The solid lines are analytical estimates obtained with Eq.(S16).

that full maturation occurs after a time t_{mat}, One may defined N_{ves} and N_{mat} as:

$$N_{ves} = \int_0^{t_{mat}} K N_B(t) dt \qquad N_{mat} = N_B(t_{mat}) \tag{S16}$$

where $N_B(t)$ is assumed to follow the mean-field evolution given by Eq.(S17). This estimate, shown as solid lines in Fig.S2, accurately reproduces the observed distribution. This suggests that, for the parameters of Fig.S2, the main source of fluctuation comes from the distribution of the isolation time t_{mat}.

S5.3 Role of homotypic fusion: Linear stability analysis of the steady-state

The mean-field equations, in the presence of homotypic fusion and cooperative maturation, read:

$$\begin{gathered} \dot{A} = n_v J(\phi) - J_m \quad \text{and} \quad \dot{B} = J_m - n_v K B \\ \text{with} \quad J(\phi) = J_0(1-\phi) \quad \text{and} \quad J_m = k_m A(1+\alpha\phi) \end{gathered} \tag{S17}$$

with $\phi = \frac{B}{A+B}$.

In the following, we normalise rates by the budding rate: $j_0 = J_0/K$ and $\bar{k}_m = k_m/(n_v K)$. One fixed point of these equations is $A = B = 0$, the other satisfies the equations:

$$A = \frac{B^2}{j_0 - B} \qquad \bar{k}_m \alpha B^2 - (1 + \bar{k}_m(1+\alpha)) j_0 B + j_0^2 = 0 \tag{S18}$$

A non-zero fixed point always exists, given by:

$$A = \frac{B^2}{j_0 - B} \qquad B = \frac{j_0}{2\bar{k}_m \alpha}\left(1 + \bar{k}_m(1+\alpha) - \sqrt{1 + 2\bar{k}_m(1-\alpha) + \bar{k}_m^2(1+\alpha)^2}\right) \tag{S19}$$

This fixed point is always stable, but one can show that the kinetics toward the fixed point is overdamped only if

$$\begin{aligned} -2(\alpha+1)^3\bar{k}_m^3 + \left(5\alpha^2 + 2\alpha - 2\right)\bar{k}_m^2 - 4\alpha\bar{k}_m + 1 > \\ 2\bar{k}_m\left((\alpha+1)^2\bar{k}_m - \alpha\right)\sqrt{\bar{k}_m\left(-2\alpha + (\alpha+1)^2\bar{k}_m + 2\right) + 1} \end{aligned} \tag{S20}$$

This means that there is a decreasing function $\bar{k}_{m,\mathrm{crit}}(\alpha)$ (shown in Fig.S3, and whose maximum is $\bar{k}_{m,\mathrm{crit}}(0) \simeq 0.42$) such that when $\bar{k}_m > \bar{k}_{m,\mathrm{crit}}(\alpha)$ the system reaches the steady-state undergoing oscillations. The larger $\bar{k}_m$, the closer the oscillations bring the system to the full maturation adsorbing boundary $A = 0$. The full maturation probability thus becomes relatively independent on the system's size in that case. Note that this behaviour rely mostly on the existence of homotypic fusion, and can in principle be observed in the absence of cooperativity $\alpha = 0$, although cooperativity does decreases the threshold $\bar{k}_{m,crit}$ beyond which relaxation is underdamped.

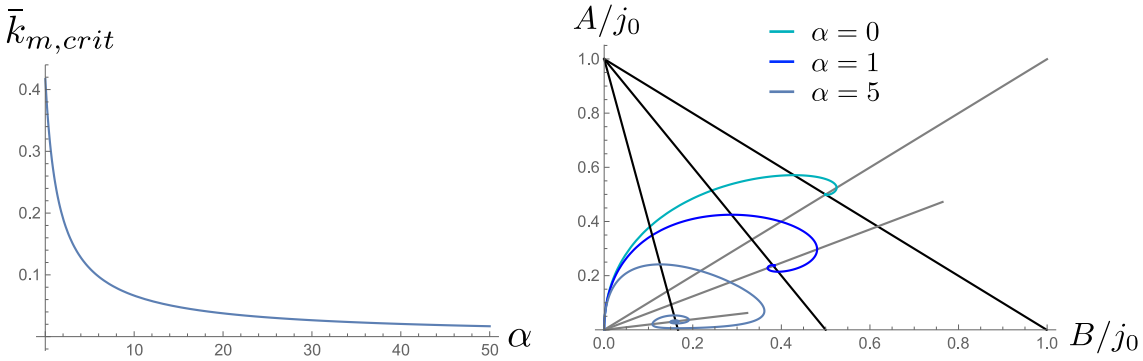

Figure S3: Left, Value of the critical maturation rate $\bar{k}_{m,\mathrm{crit}}$ beyond which the system shows damped oscillations around the fixed point. Right. Trajectories in the phase space $\{A(t), B(t)\}$ for $\bar{k}_m = 1$ and different values of α ($= 0,\ = 1,\ = 5$). The black (gray) lines are the corresponding null clines $\dot{A} = 0$ ($\dot{B} = 0$).

S5.4 Phase diagrams for the full model.

In the full model, the fluxes characterising the influx of immature (A) components, their maturation into mature (B) components, and the exit of B components, are written, respectively:

$$\begin{aligned} J_{A,in} = J(N,\phi)n_v \quad , \quad J_{A\to B} = k_m(\phi)N_A \quad , \quad J_{B,out} = K(\phi)n_v N_B \\ J(N,\phi) = N^\beta(1-\phi) \quad , \quad k_m(\phi) = k_m(1+\alpha\phi) \quad , \quad K(\phi) = K\phi \end{aligned} \tag{S21}$$

where the parameter β quantifies the size dependence of the influx and the parameter α quantifies the cooperativity of the maturation process. Fig.S4 shows different phase diagrams varying these parameters. It complements the Fig4 of the main text, which only shows transition boundaries for $\eta - 0.5$. In addition, it explores the case where the influx depends on the size of the compartment: $\beta = 1/2$, which corresponds to a diffusion-limited fusion of the vesicular influx. The main result

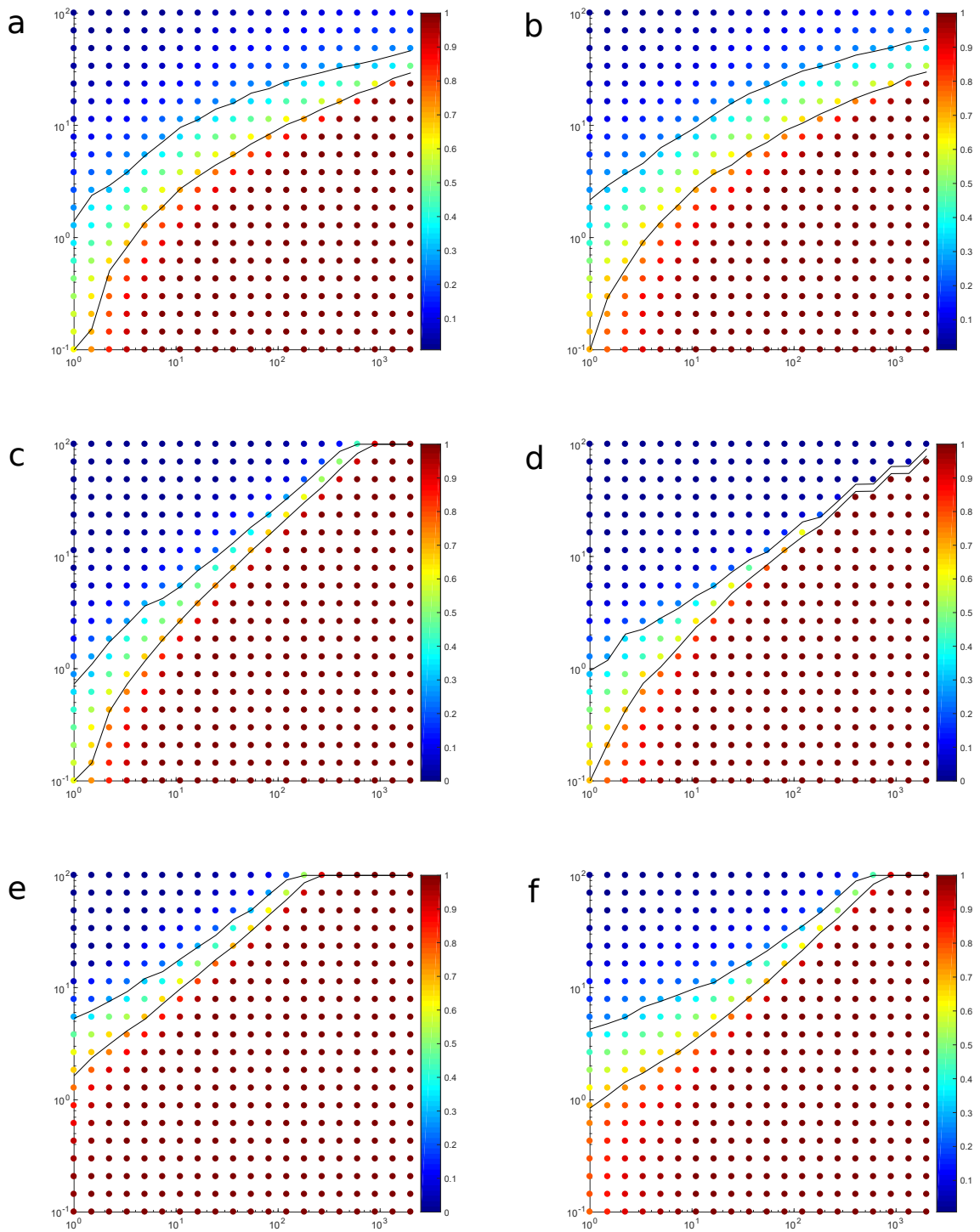

Figure S4: Phase diagram for the output parameter η as in Figs.2-3 of the main text, for different values of the parameters of the full model: **a**. $J = J_0(1-\phi)$, $n_v = 1$ **b**. $J = \sqrt{N}J_0(1-\phi)$, $n_v = 1$ **c**. basic model, **d**. $J = J_0\sqrt{N}$, $n_v = 1$ **e**. $n_v = 10$ and **f**. $k_m(\phi) = k_m(1+\alpha\phi)$ with $\alpha = 50$, $n_v = 1$.

is that the width of the transition is mostly influenced by the mechanism of homotypic fusion. The transition is smoother when homotypic fusion is treated in a continuous manner ($J \sim (1-\phi)$ - Fig.S4a,b). This reflects the fact that in the former case, full compartment maturation is an almost deterministic process that occurs during the first oscillation, hence lacks the exponential nature related to stochasticity. One the other hand, a size dependent influx makes little difference to the phase diagram (compare Fig.S4 a and b, or Fig.S4 c and d).

Supporting references

[1] N. G. Van Kampen. *Stochastic Processes in Physics and Chemistry.* Elsevier, 2007.

[2] D.T. Gillespie. Exact stochastic simulation of coupled chemical reactions. *J. Chem. Phys.*, 81(25):2340–2361, 1977.